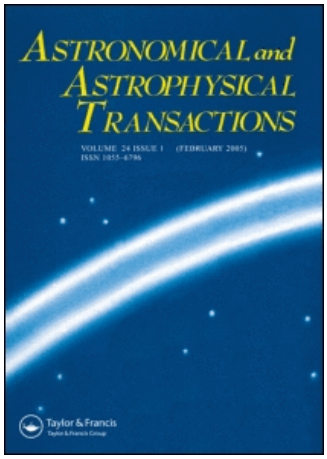

Astronomical & Astrophysical Transactions
The Journal of the Eurasian Astronomical Society
Publication details, including instructions for authors and subscription information:
http://www.informaworld.com/smpp/title~content=t713453505

Interplanetary scintillation using EISCAT and MERLIN: extremely long baselines at multiple frequencies

R. A. Fallows [a]; A. R. Breen [a]; M. M. Bisi [a]; R. A. Jones [a]; G. D. Dorrian [a]
[a] Institute of Mathematical and Physical Sciences, University of Wales, Wales, UK

Online Publication Date: 01 December 2007
To cite this Article: Fallows, R. A., Breen, A. R., Bisi, M. M., Jones, R. A. and Dorrian, G. D. (2007) 'Interplanetary scintillation using EISCAT and MERLIN: extremely long baselines at multiple frequencies', Astronomical & Astrophysical Transactions, 26:6, 489 - 500
To link to this article: DOI: 10.1080/10556790701612197
URL: http://dx.doi.org/10.1080/10556790701612197

Astronomical and Astrophysical Transactions
Vol. 26, No. 6, December 2007, 489–500

Interplanetary scintillation using EISCAT and MERLIN: extremely long baselines at multiple frequencies

R. A. FALLOWS*, A. R. BREEN, M. M. BISI, R. A. JONES and G. D. DORRIAN

Institute of Mathematical and Physical Sciences, University of Wales,
Aberystwyth SY23 3BZ, Wales, UK

(Received 19 July 2007)

Improvements to two of the radio telescopes of European Incoherent SCATter radar (EISCAT) allow measurements of Interplanetary Scintillation (IPS) at 1.4 GHz, and this has prompted two major developments in studies of IPS. Simultaneous observations between EISCAT and MERLIN allow baselines of up to 2000 km, significantly improving velocity resolution and making possible much greater accuracy in determining the direction of flow than previously, as well as demonstrating that density variations in the slow solar wind remain partially correlated for at least 8 s. Initial results suggest two fast solar wind modes, and there is evidence for super-radial (meridional) expansion of the fast solar wind. Trials have been conducted using different observing frequencies at different sites, including the use of the EISCAT Svalbard Radar for IPS for the first time. Observations at 500, 928 and 1420 MHz with baselines of up to 1200 km have been carried out. The results are found to be consistent between single- and dual-frequency correlations, allowing the range of observations possible with the EISCAT system to be expanded.

Keywords: Solar wind; Interplanetary scintillation; Coronal mass ejections

1. Introduction

Interplanetary scintillation (IPS) arises from the scattering of radio waves from a distant, compact source by density variations within the solar wind. The three antennas of the European Incoherent SCATter radar (EISCAT) have made such measurements to probe the solar wind at all heliographic latitudes over distances ranging from $15R_{\odot}$ to more than $100R_{\odot}$ since 1982 [1] and on a regular basis since 1990. Simultaneous observations using all three of the EISCAT antennas allow a cross-correlation analysis [2, 3] to be used between any antenna pair to determine the solar wind speed(s) across the line of sight.

A principle advantage of the EISCAT facility has been the long baselines (up to 390 km) available between the antennas. Increasing the separation of the antennas when projected on to the plane of the sky increases the difference in time-lag between different solar wind streams, thus improving the ability to resolve these streams in the cross-correlation function [4–6].

*Corresponding author. Email: raf@aber.ac.uk

Astronomical and Astrophysical Transactions
ISSN 1055-6796 print/ISSN 1476-3540 online © 2007 Taylor & Francis
http://www.tandf.co.uk/journals
DOI: 10.1080/10556790701612197

Observations since 1994 have consistently demonstrated that both fast and slow solar wind streams can appear as two distinct peaks in the cross-correlation function when the baseline is sufficiently large [2, 6, 7].

The cross-correlation between the scintillation patterns observed at two sites should be maximised if the projection onto the plane of the sky of the baseline between the receiving sites was parallel to the projection onto the sky plane of the solar wind outflow [8]. This approach was used [9] to detect non-radial flow in the solar wind in long-baseline EISCAT observations where the projected baseline was allowed to rotate through the radial direction.

In 2002, EISCAT was upgraded to allow measurements at an observing frequency of 1420 MHz at two of the sites [10]. This has lead to two main improvements in using IPS to study the solar wind. The first of these is the use of extremely long baselines: simultaneous observations between EISCAT and the MERLIN system in the UK, allowing baselines of up to ~2000 km, were first trialled in May 2002 with more extensive programmes carried out in May 2004, 2005 [11, 12] and 2006. Such observations greatly improve the ability to resolve different solar wind streams in the cross-correlation function and the sensitivity with which the flow direction of the solar wind can be determined.

The complication of a transmitting system has meant that the remaining EISCAT antenna, at Tromsø, has yet to be upgraded and still uses the original observing frequency of 928 MHz. Hence the ability to cross-correlate different observing frequencies assumes some importance in maintaining IPS observations with all of the baselines available at EISCAT. Cross-correlation between two different observing frequencies is accounted for in IPS theory [13], but has seldom been used in practice. Trial observations were carried out at EISCAT in September 2003 and in May 2004 the EISCAT Svalbard Radar (ESR) was used for the first time for IPS, increasing the available baselines to more than 1000 km [14].

This paper summarises the principle results of these trials so far and presents preliminary analyses from observations carried out in spring 2006.

2. Background theory

Density fluctuations in the solar wind, which are assumed to be of turbulent origin, cause phase variations to be introduced in the radio signal from a distant source. If the rms phase difference over transverse scales equal to the radius of the first Fresnel zone $R_\mathrm{f} = \sqrt{\lambda z/2\pi}$ are small ($\ll$1 rad), then the level of scattering is said to be 'weak' and diffraction can be modelled with the Born approximation as a linear summation of the effects of a series of 'thin screens' along the line of sight between the source and receiver. The resulting intensity fluctuations have most of their energy at scales near R_f. Since R_f changes with distance z, the line of sight integration spreads the energy over a range of scales. Higher observing frequencies, sensitive to smaller density scales, which are weaker, may be used to maintain observations within a weak scattering regime as the mean solar wind density increases closer to the Sun.

The IPS temporal power spectrum under weak scattering conditions can be expressed by the following equation [15] (and references therein):

$$P(f) = 8\pi r_\mathrm{e}^2 \lambda^2 \int_0^\infty \frac{2\pi}{v_\mathrm{p}(z)} \int_{-\infty}^{\infty} \sin^2\left(\frac{q^2\lambda z}{4\pi}\right) |V(q, z, \theta_0(\lambda))|^2 q^{-\alpha} \exp -\left(\frac{q}{q_i}\right)^2 R^{-4} \mathrm{d}q_y \mathrm{d}z \quad (1)$$

where: r_e is the classical electron radius; λ is the observing wavelength; v_p is the component of solar wind velocity perpendicular to the line of sight; q is the two-dimensional spatial wavenumber; z is the distance from the Earth to the scattering screen; $V(q, z, \theta_0(\lambda))$ is the visibility function of a radio source of size $\theta_0(\lambda)$. $\sin^2(q^2\lambda z/4\pi)$ is the Fresnel filter which acts as a high-pass filter attenuating wavenumbers below the Fresnel frequency, $q_f = \sqrt{4\pi/\lambda z}$. $\exp(-(q/q_i)^2)$ describes the dissipation and attenuates the scintillation power spectrum at wavenumbers higher than q_i. In addition, the source visibility function also acts as a low-pass filter attenuating wavenumbers above $q_s = 1/z\theta_0$.

Equation 1 assumes a single observing frequency and so only represents the auto-spectrum for each antenna in the case of dual-frequency observations. A simple modification is needed for the cross-spectrum in this case. All the λ^2 terms are separated into single λ terms and the cross-spectrum becomes [13]:

$$P(f) = 8\pi^2 r_e^2 \lambda_1 \lambda_2 \int_0^\infty \frac{2\pi}{v_p(z)} \int_{-\infty}^{\infty} \sin\left(\frac{q^2\lambda_1 z}{4\pi}\right) \sin\left(\frac{q^2\lambda_2 z}{4\pi}\right) |V(q, z, \theta_0(\lambda_1))||V(q, z, \theta_0(\lambda_2))| q^{-\alpha} \exp -\left(\frac{q}{q_i}\right)^2 R^{-4} \mathrm{d}q_y \mathrm{d}z \quad (2)$$

The assumption of weak scatter must be valid for both observing frequencies. The cross-correlation between different frequencies drops much more quickly in strong scattering than is the case for single-frequency cross-correlation, so this technique cannot be used as close to the Sun as the single-frequency case. By contrast, any radio source is limited in how far from the Sun its scintillation can be measured at a given frequency by its strength, angular size and structure. Therefore, radio sources and heliocentric distances have to be picked carefully to ensure that these restrictions are satisfied for both observing frequencies.

3. Results

The observations described in this paper were carried out in May 2004, 2005 and 2006. The principle results are summarised and preliminary results from the May 2006 observations are presented.

A weak scattering IPS model allowing for the presence of two solar wind streams in the line of sight has been used for the last decade to analyse EISCAT IPS observations [2, 3, 16]. The current analysis routines perform all fitting to the auto- and cross-power spectra, with the resulting correlation functions displayed for a more convenient visualization.

The power spectrum of the density variations in the solar wind giving rise to IPS is described by a power law with exponent α, cut off by an 'inner scale' corresponding to the dissipation scale of the turbulence. Previous studies [17] have found α to vary between 2 and 4 and the inner scale in kilometres to be roughly equal to the distance of the observation in solar radii, although it is not very well determined. We adjust these parameters to match the high-frequency tail of the auto-power spectrum. The density variations are assumed to be anisotropic and normally extended in the radial direction. The model assumes that a fast stream will be present in the central portion of the line of sight, flanked by a slow stream at either end. The slow stream is given an extra weighting to account for its greater density and hence greater

scattering power. Following the work of Little and Ekers [18], each stream can be modelled as having a mean speed with random velocity components in the radial ($\delta V_{||}$ – indicated by a skewed cross-correlation function) and transverse ($\delta V_{\perp}$ – indicated by a reduced area under the cross-correlation function) directions. The region of the IPS raypath overlying the polar coronal hole – and hence assumed to be immersed in the fast stream – is estimated by ballistically projecting the raypath down onto a white light map constructed from SOHO|LASCO observations [19].

The analysis routines have required extensive development to be used for extremely-long baselines and multiple observing frequencies. This development work is still on-going, but in this paper we also present initial analyses of the most recent results. Detailed results from the improved routines will be the subject of forthcoming papers.

3.1 *Extremely long baselines*

The first trial of simultaneous observations between MERLIN and EISCAT, allowing baselines of up to 2000 km, was carried out in May 2002. Figure 1 shows the principle results of this trial: significant correlation is seen with peaks corresponding to the fast and slow solar wind streams showing up separately and further demonstrating that density variations in the slow solar wind remain correlated to some degree for at least 8 s [11, 12].

It is possible to determine the actual outflow direction of the solar wind if the observation is made over a period of time long enough for the Earth's rotation to rotate the baseline, as

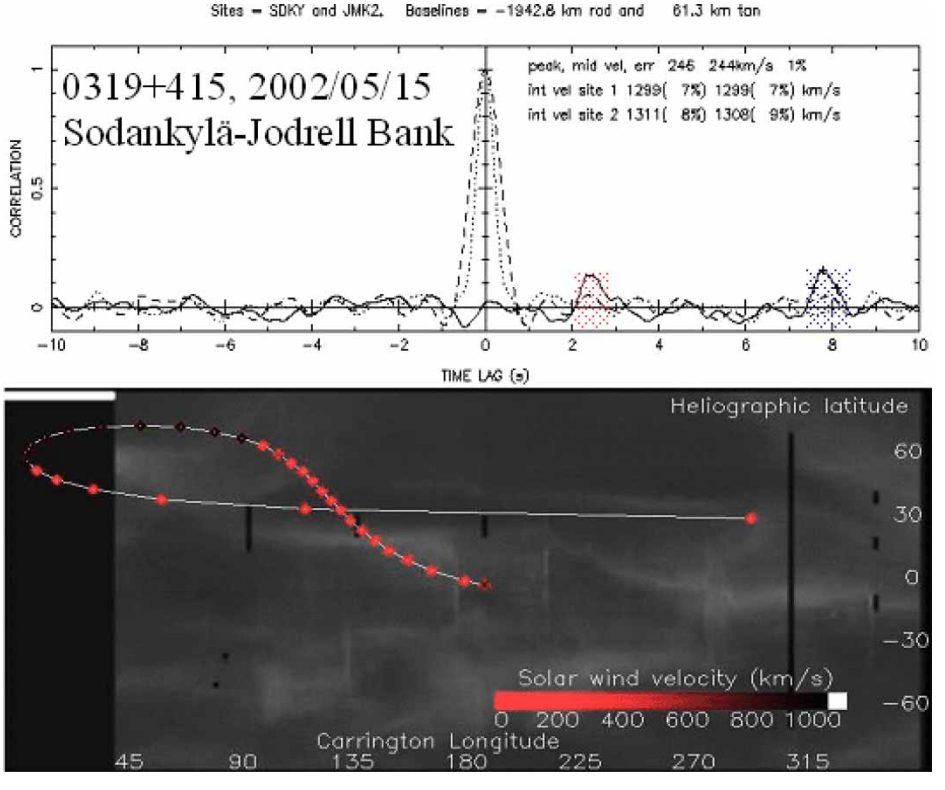

Figure 1. Correlation functions on a Sodankylä (EISCAT)–Jodrell Bank (MERLIN) baseline from an observation of 0319 + 415 on 15 May 2002.

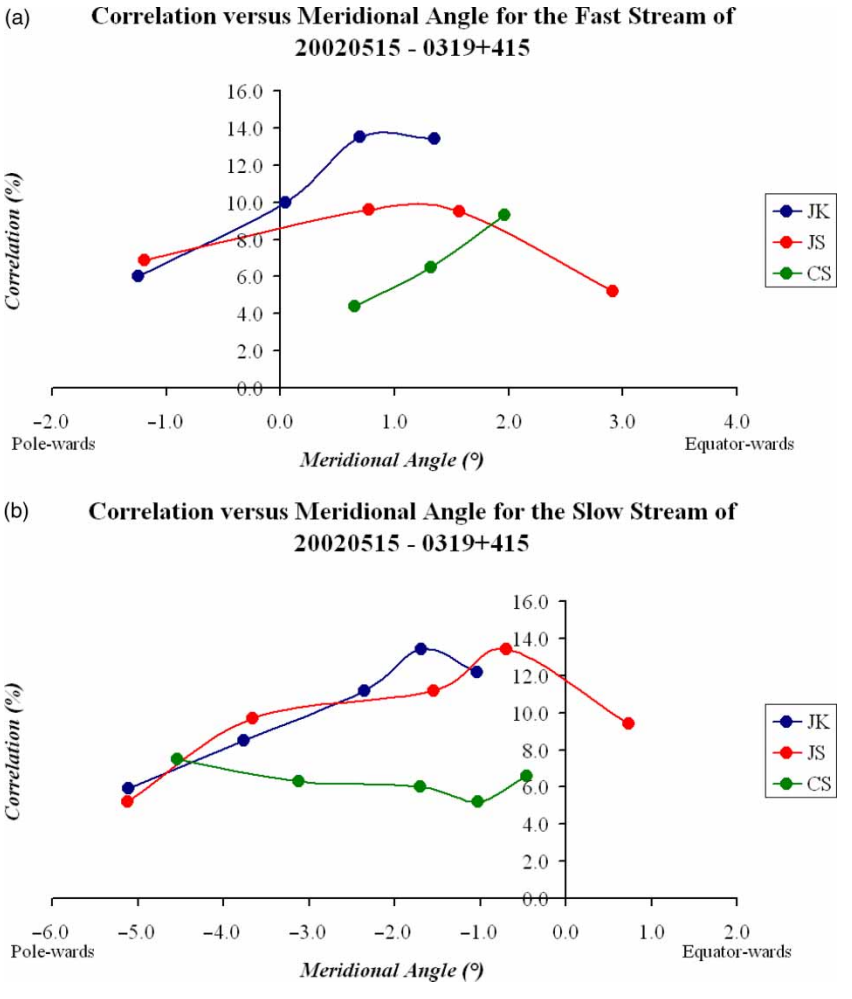

Figure 2. Plots of correlation peak height versus off-radial angle for various baselines from an observation of J0319+415 on 15 May 2002. The point of closest approach of the line of sight to the Sun was at a distance from the Sun of $83R_{\odot}$ and heliographic latitude of 60°.

projected onto the sky plane, through the radial direction from the Sun [9, 12]. During such an observation, the height of the cross-correlation peak will increase as the true flow direction is approached, and decrease again subsequently.

This approach was originally used for EISCAT observations in the mid-1990s [9]. In these observations a small, but significant, off-radial flow component was detected. However, the flow direction was found to be only 1° to 3° off-radial which meant a Monte Carlo analysis had to be used to determine its significance, given the shorter baselines available.

The much longer baselines available between EISCAT and MERLIN mean that off-radial flow can be detected much more easily, with greater sensitivity, and without the need for Monte-Carlo statistics. Figure 2 shows the variation with off-radial angle of the cross-correlation peak height for both the fast and slow stream peaks seen in the May 2002 observation of J0319+415 [12].

A small equatorwards deviation of 1° to 2° is seen in the fast stream whereas a small polewards deviation of a similar order is seen in the slow stream. This suggests a slight overexpansion to lower latitudes in the fast stream and this is further confirmed by several

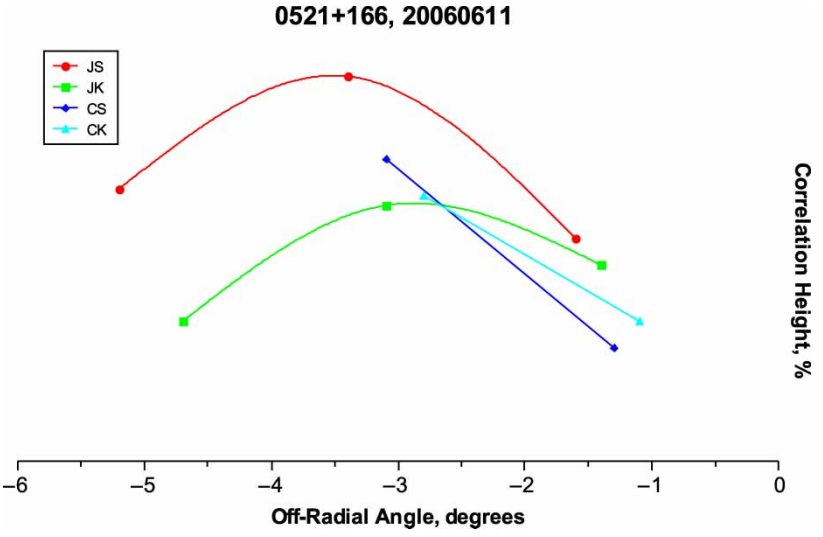

Figure 3. Plot of correlation peak height versus off-radial angle for various baselines from an observation of J0521+166 on 11 June 2006. The point of closest approach of the line of sight to the Sun was at a distance from the Sun of $24R_{\odot}$ and heliographic latitude of $-81°$.

similar observations since [12, 20]. However, the slow stream result has yet to be confirmed by further observations and it is not certain whether the deviation seen is due to a genuine overexpansion or is the result of a weak interaction deflecting the flow northward.

All the extremely long baseline observations to 2006 dominated by fast solar wind have involved northern solar hemisphere radio sources. In June 2006, the first such observations of a southern hemisphere source at high solar latitudes were carried out. Preliminary analysis shows that the fast solar wind appears to be expanding equatorwards (figure 3), confirming that the southern hemisphere fast wind seems to be symmetric with that of the northern hemisphere.

Several high-latitude EISCAT IPS observations from the last solar minimum appeared to fit better on analysis by assuming that the fast wind had two modes, a 'fast' mode and a 'faster' mode with the 'faster' mode found above the polar crown and the 'fast' mode lying above the lower-latitude extents of the polar coronal hole [21]. The weak scattering model described above has been extended to allow for a second fast wind mode, assumed to lie above the lowest latitudes of the polar coronal hole.

The cross-correlation functions of some high-latitude extremely long baseline observations have shown two distinct peaks at time lags corresponding to the fast solar wind, thus giving a much stronger indication of the presence of two modes. The observation of J0521+166 on 11 June 2006 is an example. Figure 4 gives the average auto-correlation function and stacked cross-correlation functions for various baselines, complete with a preliminary model fit using the weak scattering model described above and assuming two modes of fast solar wind.

In this analysis, the locations of slow and fast wind were estimated from the white light map given in figure 4. Reasonable values were used for most parameters quoted; only the faster and fast velocities and the width of the fast mode were fitted using a least-squares routine. An off-radial flow direction of 2° was found to model the cross-correlation functions better, close to the 3° value estimated from plotting cross-correlation function height versus off-radial angle. It is likely that the faster wind velocity of 904 km s^{-1} is an over-estimate as there is little to suggest the presence of a Coronal Mass Ejection (CME) or other feature that may allow for such a speed at this distance from the Sun.

Coronal Mass Ejections can be detected in IPS measurements: Usually there are one or more signatures indicating their presence in the line of sight [3, 16, 22], including a quick change in

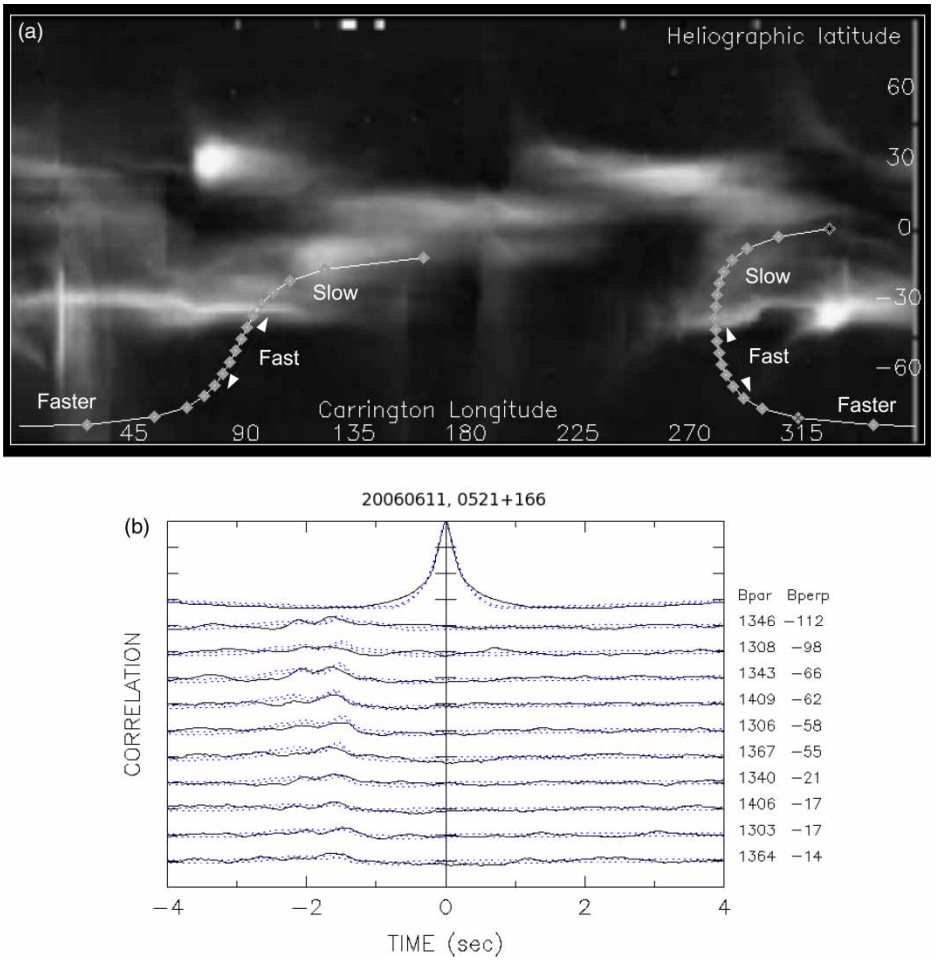

Figure 4. Top: Synoptic map of white light at a height of $2.5R_{\odot}$ from LASCO measurements. The IPS line of sight is mapped balistically down to this height and over-plotted. The modelled extent of the fast wind in the line of sight is shown, with slow wind assumed equatorward of this and faster wind assumed poleward of it. Bottom: Average auto-correlation (top) and stacked cross-correlation functions for various baselines. Each cross-correlation function was created using a 10-min segment of data with the start time advanced every 5 min. The solid lines give the data and the dual dotted lines give the model fit. Parameters are: $V_{\rm faster}$, 904 km s^{-1}; $V_{\rm fast}$, 691 km s^{-1}; axial ratio, 2.5; $V_{\rm slow}$, 350 km s^{-1}; weighting, 5.3; α, 3.0; inner scale, 24.0; fast stream width, 29°; fast streams off-radial angle, 2°.

the shape of, or features in, the cross-correlation function. Observations of J0319+415 carried out on 13 and 14 May 2005 are an excellent example of a likely CME.

IPS measurements of J0319+415 on 13 May 2005 were seen to undergo a significant and highly variable enhancement of signal strength at all EISCAT and MERLIN sites between ∼1630 and 1715UT (figure 5). This unusual variation appeared to be simultaneous between all sites. Comparison with measurements from the Phoenix-2 radio spectrometer confirmed that the anomalous signal was the result of a coronal radio burst, co-temporal with a solar flare, detected in the relatively flat, off-axis response of the radio telescopes [23].

A CME associated with this event was seen in LASCO white light and observed to pass through the IPS line of sight of the observation of J0319+415 on 14 May 2005 [22]. The CME is easily identifiable in the cross-correlation functions (figure 6): the twin-peak features seen in the top four cross-correlation functions were all seen in the previous days observation of the same source, indicating that they represent the background solar wind. The single-peak

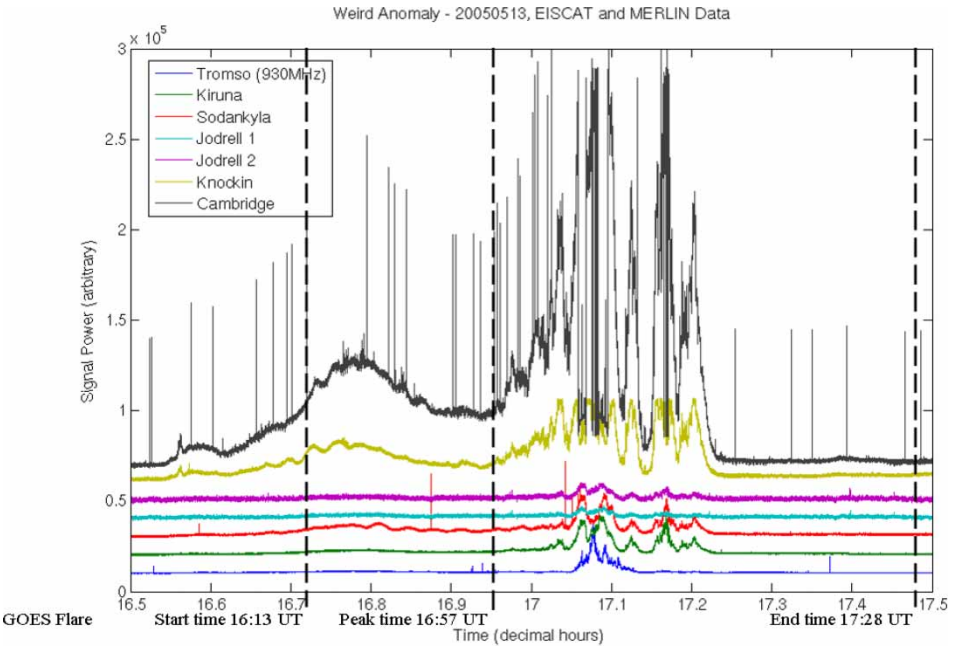

Figure 5. Observations from EISCAT and MERLIN of the anomalous radio signal strength enhancement of 13 May 2005. The Jodrell Bank (Mk.1A), Cambridge and Knockin telescopes of MERLIN and the Kiruna and Sodankyl telescopes of EISCAT were operating at a central frequency of 1.4 GHz. The Troms telescope of EISCAT was operating at a central frequency of 0.93 GHz.

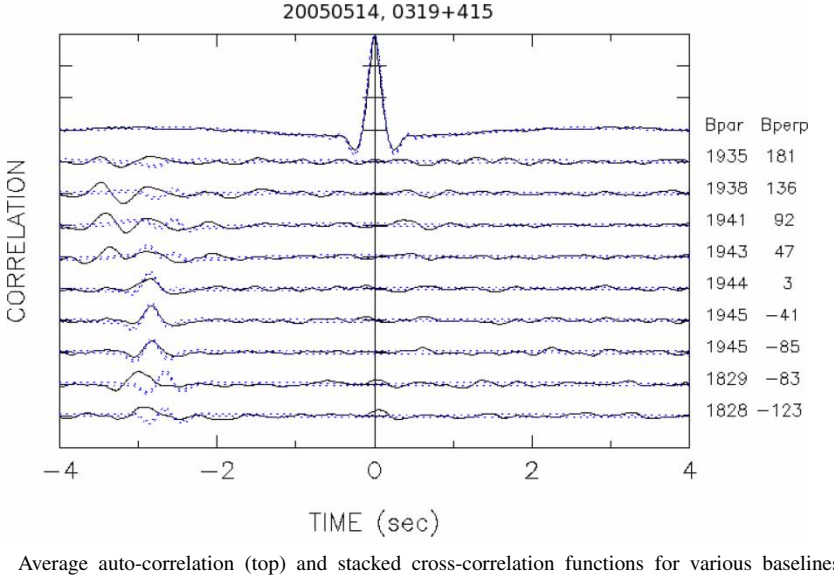

Figure 6. Average auto-correlation (top) and stacked cross-correlation functions for various baselines. Each cross-correlation function was created using a 10-min segment of data with the start time advanced every 5 min. The solid lines give the data and the dual dotted lines give the model fit. Parameters are: V_{CME} 690 km s^{-1} (assumed to be in the Earthward half of the line of sight; V_{fast} 763 km s^{-1} (occupying the remaining portion of the line of sight); axial ratio 0.9; fast stream weighting 0.4; α 2.0; inner scale 83.0; off-radial angle of CME 10 polewards.

feature seen in the remaining functions was not observed the previous day and so can only be assumed to be a result of a transient feature. The launch time and speed of the CME seen in LASCO the previous day makes it the ideal candidate for this transient feature.

An attempt (also given in figure 6) has been made to model this observation. Since the CME was observed passing the Advanced Composition Explorer (ACE) spacecraft on 15 May 2005, and it was observed as a front-sided halo in LASCO, this modelling attempt assumes that the CME occupies the Earthward half of the line of sight, from the point of closest approach. The fast stream is then assumed to occupy the remainder of the line of sight. The result is far from perfect, but some of the cross-correlation peaks corresponding to the CME are matched by the model, with an off-radial flow direction 10° polewards found to fit the CME best. This agrees with plots of cross-correlation height versus off-radial angle made using these measurements [12, 20].

3.2 *Multiple observing frequencies*

Due to the complication of a transmitting system at the Tromsø EISCAT site, this site has not been upgraded to allow observations to be carried out at 1420 MHz. Since GSM interference at the Sodankylä has reduced the usable bandwidth at the old observing frequency of 928 MHz to less than is useful for IPS, observations here must be carried out 1420 MHz. Hence to maintain the full range of baselines available at EISCAT, it is necessary to cross-correlate two different observing frequencies. A further advantage of this is increasing the flexibility of our IPS observations by the ability to use other radio antennas which would not be available

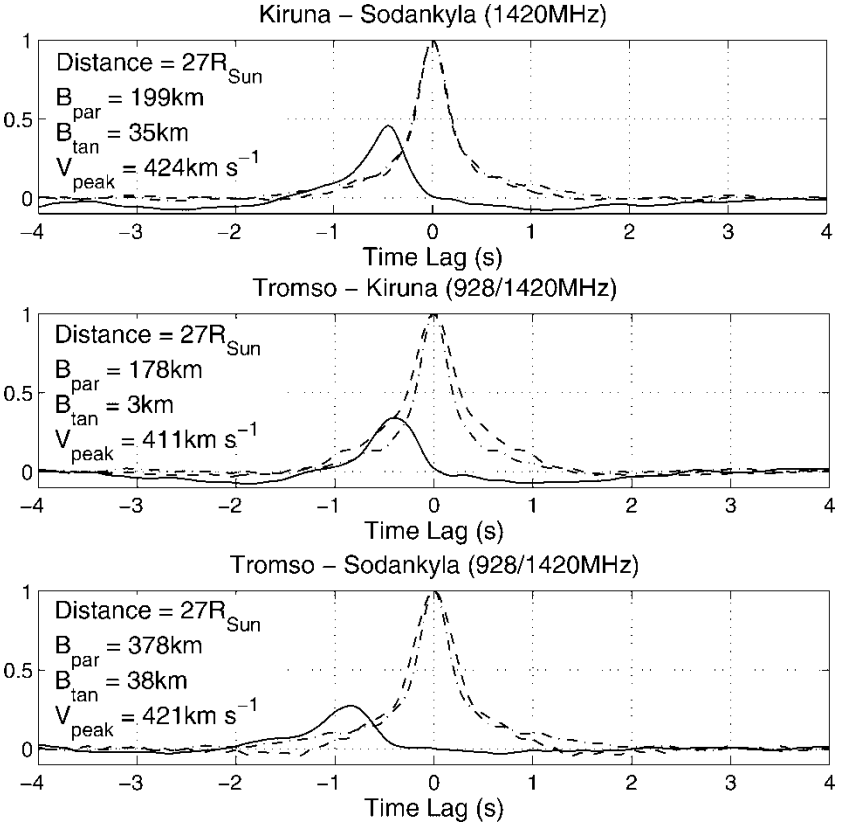

Figure 7. Auto- and cross-correlation functions for an observation of J1256−057 on 1st October 2003. Auto-correlation functions are represented by dashed lines and dash-dotted lines for the first and second antennas, respectively, in each plot. Cross-correlations are represented by solid lines.

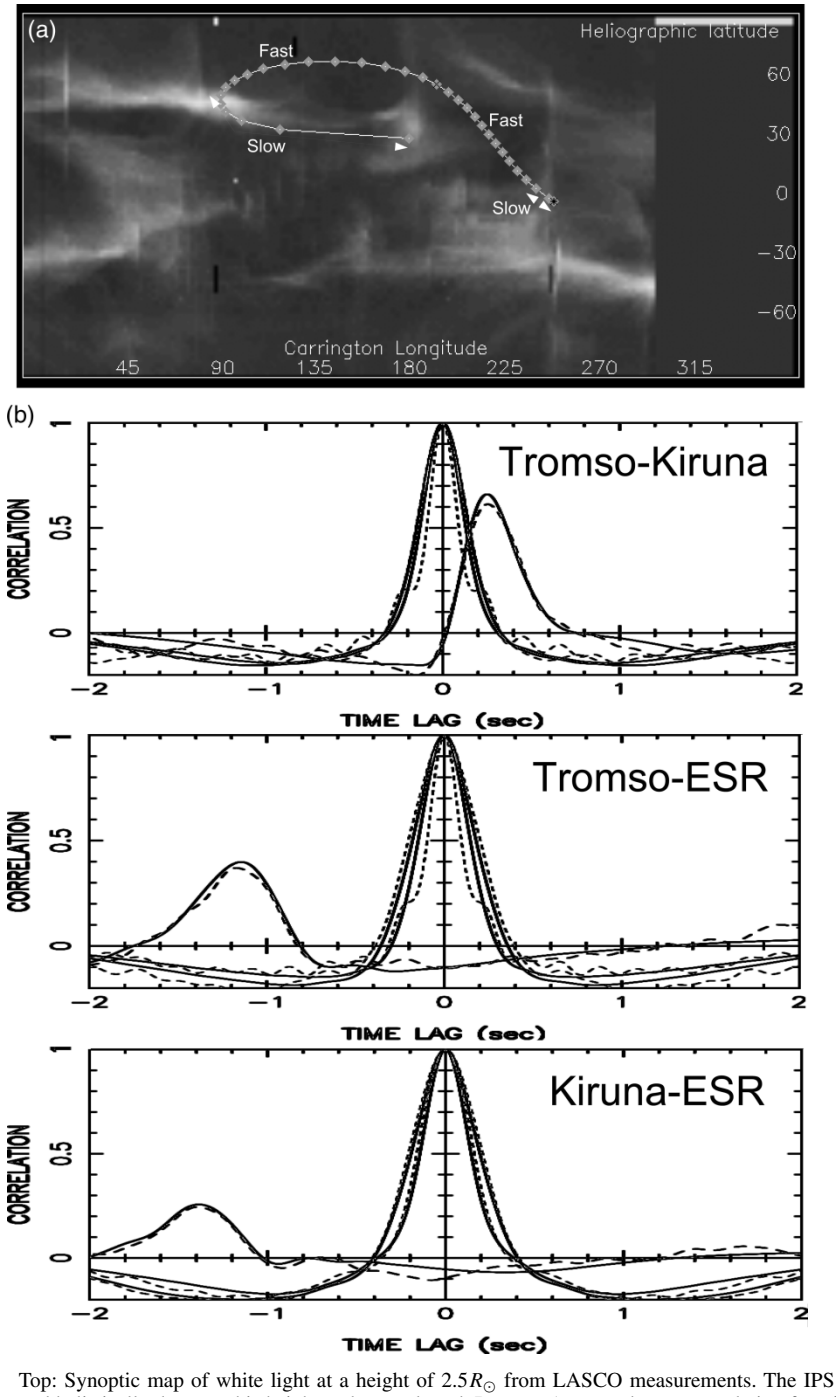

Figure 8. Top: Synoptic map of white light at a height of $2.5R_{\odot}$ from LASCO measurements. The IPS line of sight is mapped balistically down to this height and over-plotted. Bottom: Auto- and cross-correlation functions for an observation of J0319+415 on 12th May 2004. A two-stream model fit is also included: the data are represented by dashed lines; solid lines represent the model correlations. Parameters are: $V_{\rm fast}$ 775 km s^{-1} with dV$_{||}$ 250 km s^{-1}; $V_{\rm slow}$ 400 km s^{-1} with weighting 8; axial ratio 1.8; α 3.0; inner scale 85.0.

otherwise. An example of this is the ESR, which operates at a frequency of 500 MHz. The first dual-frequency observations were trialled in September 2003 with use of the ESR, providing baselines of up to 1200 km within the EISCAT system, trialled in May 2004 [14].

Figure 7 shows an EISCAT observation of J1256−057 on 1st October 2003. The receivers at both Kiruna and Sodankylä were set at 1420 MHz, while the receiver at Tromsø remained at 928 MHz.

The time lags of the cross-correlation functions indicate that a slow stream of $\sim$400 km s^{-1} dominates in this observation, although the extension of the cross-correlation functions to longer time lags indicate the presence of another, slower, stream as well. Cross-correlations between the two observing frequencies are slightly reduced and broadened compared to the single-frequency case. The level of correlation between two different frequencies is expected to be lower than the level at a single frequency as the range of density scales giving rise to the scintillation at each frequency is not exactly the same.

Use of the ESR from May 2004 adds a third observing frequency (500 MHz) to the EISCAT system over baselines of up to 1200 km. Figure 8 shows the correlation functions between all three observing frequencies for an observation of J0319+415 carried out on 12th May 2004.

A preliminary fit – the first attempt to model EISCAT multi-frequency correlations – using a two-stream weak scattering model modified to account for two observing frequencies in the cross-correlation function has been carried out. Reasonable values have been used for most parameters with only the mean fast stream velocity and associated radial random component ($\mathrm{d}V_{||}$) fitted with a least-squares fitting routine. The results provide a good fit to all three cross-correlation functions, each involving a different pair of frequencies, giving confidence to the dual-frequency model.

4. Conclusions

Extremely long baseline IPS observations provide the most precise resolution of remote sensing measurements to date of different solar wind streams in the line of sight, and also provide a straightforward method of determining their flow direction.

The flow direction of the fast solar wind is found to be 1° to 3° off-radial in all extremely-long baseline observations to date. These observations have mostly been at northern solar latitudes and have all shown an equatorward expansion. A preliminary analysis of the first such observations at high southern solar latitudes have also indicated an equatorward expansion, providing symmetry between both solar hemispheres. Preliminary analysis of these results using a two-stream weak scattering model appear to confirm the flow directions found using simple plots of cross-correlation height.

The radio burst from a solar flare has been detected simultaneously in the far off-axis response of the antennas from two independent systems. A CME was associated with this event, and this CME was observed to pass through the IPS line of sight the following day. Preliminary analysis with the weak scattering model seems to confirm that the flow direction of the CME is $\sim$10° off-radial in a polewards direction.

A clear correlation is seen between measurements of IPS carried out at different observing frequencies. The level of correlation depends on how much overlap there is between the density scales observed with each frequency. This will restrict the difference between observing frequencies over which it is possible to obtain correlation for a particular baseline. Nevertheless a high degree of correlation exists between frequencies differing by almost a factor of 3, with a time lag of 1.5–2 s.

The first preliminary analysis of dual-frequency correlations using a modified weak scattering model have been carried out. This demonstrates a clear consistency between analyses involving three different frequencies and the results are in line with those expected from single-frequency measurements.

References

[1] G. Bourgois, W. Coles, G. Daigne *et al.*, Astron. Astrophys. **144** 452 (1985).
[2] W. Coles, Astrophys. Space Sci. **243** 87 (1996).
[3] A. Canals, A. Breen, P. Moran *et al.*, Ann. Geophys. **20**(9) 1265 (2002).
[4] R. Grall, Remote sensing observations of the solar wind near the sun, PhD. thesis, University of California, San Diego (1995).
[5] A. Rao, A. Pramesh, V. Balasubramanian *et al.*, in Proceedings of the International Solar Wind 8 Conference, (1995), p. 94. Dana Point, California.
[6] R. Grall, W. Coles, M. Klinglesmith *et al.*, Nature **379** 429 (1996).
[7] A. Breen, W. Coles, R. Grall *et al.*, Ann. Geophys. **14** 1235 (1996).
[8] A. Breen, W. Coles, R. Grall *et al.*, J. Atm. Terr. Phys. **58**(1–4) 507 (1996).
[9] P. Moran, A. Breen, C. Varley *et al.*, Ann. Geophys. **16** 1259 (1998).
[10] G. Wannberg, L.-G. Vanhainen, A. Westman *et al.*, in Proc. Union of Radio Scientists (URSI) Maastricht, Netherland (2002).
[11] A. Breen, R. Fallows, M. Bisi *et al.*, J. Geophys. Res. **111**(A8) A08104 (2006).
[12] M. Bisi, A. Breen, R. Fallows *et al.*, in Solar Wind 11 – SOHO 16, ESA SP-592, edited by B. Fleck and T. Zurbuchen, (2005), p. 593.
[13] E. Salpeter. Astrophys. J. **147**(2), 433 (1967).
[14] R. Fallows, A. Breen, M. Bisi *et al.*, Geophys. Res. Lett. **33** L11106 (2006) DOI: 10.1029/2006GL025804.
[15] S. Scott, B. Rickett and J. Armstrong, Astron. Astrophys. **123** 191 (1983).
[16] M. Klinglesmith, The polar solar wind from 2.5 to 40 solar radii: results of intensity scintillation measurements, PhD. thesis, University of California, San Diego (1997).
[17] Y. Yamauchi, M. Kojima, M. Tokumaru *et al.*, J. Geomag. Geoelectr. **48** 1201 (1996).
[18] L.T. Little and R.D. Ekers, Astron. Astrophys. **10** 306 (1971).
[19] A. Breen, P. Moran, P. Williams *et al.*, Adv. Space Res. **26**(5) 789 (2000).
[20] A. Breen, M. Bisi, R. Fallows *et al.*, Submitted to Astrophys. J. Lett. (2007).
[21] M. Bisi, R. Fallows, A. Breen *et al.*, accepted subject to minor revisions for publication in J. Geophys. Res. **112**(A6) (2007).
[22] R. Jones, A. Breen, A. Canals *et al.*, accepted for publication in J. Geophys. Res. (2007) (in press).
[23] R. Jones, A. Breen, R. Fallows *et al.*, Ann. Geophys. **24**(9) 2413 (2006).